Colloids and Surfaces B: Biointerfaces 103 (2013) 566–571

Contents lists available at SciVerse ScienceDirect

Colloids and Surfaces B: Biointerfaces

journal homepage: www.elsevier.com/locate/colsurfb

Direct electron transfer from glucose oxidase immobilized on an overoxidized polypyrrole film decorated with Au nanoparticles

Behzad Haghighi*, Mahmoud Amouzadeh Tabrizi

Department of Chemistry, Institute for Advanced Studies in Basic Sciences, P.O. Box 45195-1159, Gava Zang, Zanjan, Iran

ARTICLE INFO

Article history:
Received 19 September 2012
Received in revised form 7 November 2012
Accepted 13 November 2012
Available online 23 November 2012

Keywords:
Direct electron transfer
Glucose oxidase
Glucose biosensor
Overoxidized polypyrrole
Au nanoparticles

ABSTRACT

An overoxidized polypyrrole (OOPPy) film was electrodeposited on a glassy carbon electrode (GCE) and the modified electrode (GCE/OOPPy) was then decorated with Au nanoparticles (nanoAu). Glucose oxidase was immobilized on the surface of nanoAu decorated OOPPy modified GCE to fabricate a novel glucose biosensor (GCE/OOPPy-nanoAu/GOx). Cyclic voltammetry, electrochemical impedance spectroscopy (EIS) and scanning electron microscopy (SEM) were used to characterize the modified electrodes. A pair of well-defined redox peaks with a formal potential ($E^{\circ\prime}$) of −0.449 V and a peak to peak separation (ΔE_p) of 28 mV was observed for the direct electron transfer (DET) of the immobilized GOx. The electron transfer rate constant (k_s) was calculated to be 10.3 s^{-1}. The fabricated glucose biosensor was employed for the determination of glucose in the concentration range between 1 and 8 mM using cyclic voltammetry and amperometry. The results clearly demonstrate that nanoAu decorated OOPPy film is an excellent biocompatible scaffold for the immobilization of GOx and fabrication of a glucose biosensor.

1. Introduction

Diagnosis of various diseases by monitoring of biochemical compounds in the body fluids is essential not only for controlling of diseases but also for improving the quality of our lives. It is well known that the diabetes mellitus is one of the leading causes of death and disability in the world which can be easily diagnosed and managed by the determination of blood glucose. The great importance of glucose monitoring led to a considerable amount of fascinating research and innovative detection strategies. But, the most of the proposed strategies are relatively expensive, time consuming and involve complicated procedures. So, there is an increasing demand for the determination of glucose using inexpensive, rapid and reliable methods.

Biosensor is an analytical device which includes a biological element and a suitable transducer for the selective and quantitative determination of the specific compound in a given biological environment. The biological element binds or reacts specifically with the target compound (analyte) and generates a biological event. The transducer then converts the biological event into an analytical signal such as electrical or optical signal. A quick survey on recent studies shows that the enzyme-based electrochemical biosensors are the most cited and widely used biosensors because of their simplicity, speed of their measurement and ease of their uses. The biological element in an enzyme-based electrochemical biosensor is an enzyme which selectively reacts with the target analyte and an electrochemical transducer produces an electrical signal resulting from the electrochemical process related to the enzymatic reaction. The enzyme can be retained in an enzyme-based electrochemical biosensor using various immobilization methods [1] on different types of conducting materials which can be served as a support for the immobilization.

Conducting polymers have received considerable attention over the last two decades because of their unique physical and chemical properties and various applications in many research areas. It has been shown that conducting polymers are very suitable matrix for the fabrication of electrochemical biosensors with attractive features such as fast response time, high sensitivity and great versatility [2–8]. Polypyrrole (PPy) is one of the most extensively used conducting polymers in biosensors fabrication owing to its good electrical conductivity, stability, biocompatibility, redox properties and relative ease oxidation of its monomer (pyrrole) [9–11]. There are two chemical and electrochemical polymerization methods generally used to synthesize PPy at the electrode surface from the aqueous or organic solutions [12–14]. But, the electrochemical synthesis is more beneficial, since in addition to the chemical parameters (monomer concentration, pH, etc.), electrochemical parameters (current density, applied potential, electrolyte solution, etc.) can be varied to have a better control on the properties of the coated layer [15]. Additionally, the electropolymerized polymers show better conducting property and long-term stability for conductivity [16]. PPy film can be overoxidized at high anodic

* Corresponding author. Tel.: +98 241 415 3126; fax: +98 241 415 3232.
E-mail address: haghighi@iasbs.ac.ir (B. Haghighi).

0927-7765/$ – see front matter © 2012 Elsevier B.V. All rights reserved.
http://dx.doi.org/10.1016/j.colsurfb.2012.11.010

potentials [17–19] to produce overoxidized PPy (OOPPy) film with permselective and antifouling properties resulting from the introduction of carbonyl groups into the polymer backbone during the course of overoxidation process.

The introduction of metal nanoparticles (NPs) as a new class of compounds with unique electronic, optical, magnetic and catalytic properties offers an opportunity for the fabrication of novel biosensors. Metal NPs in comparison with their bulk counterparts provide a larger surface-to-volume ratio, higher surface reaction activity, higher catalytic efficiency and stronger adsorption ability. Also, metal NPs can interact with some biological species efficiently and facilitate their charge transfer properties [20]. It seems decoration of PPy or OOPPy with metal NPs leads the creation of new nano-hybrid materials with the integrated properties of two components. Additionally, it seems the application of OOPPy decorated with metal NPs for the fabrication of new type electrochemical biosensors can greatly enhances the electroanalytical performance of the fabricated biosensors. The application of PPy [21–30] and metal NPs-PPy composites [31,32] for the fabrication of electrochemical based glucose biosensor has been reported previously. But to the best of our knowledge few reports on the application of OOPPy [33–35] and no report on the application of metal NPs-OOPPy composite (hybrid) have been presented for the fabrication glucose biosensor. Additionally, no report has been presented for DET transfer reaction of glucose oxidase on the mentioned conducting materials.

In the present study, a PPy film was electrodeposited on the surface of a glassy carbon electrode. Thereafter, PPy film was overoxidized and decorated with Au nanoparticles electrochemically to produce a novel nano-hybrid film at the surface of GCE. The sensor (GCE/OOPPy-nanoAu) was then modified with glucose oxidase (GOx) to fabricate a novel glucose biosensor (GCE/OOPPy-nanoAu/GOx). Cyclic voltammetry studies showed a pair of well-defined redox peaks as a result of direct electron transfer (DET) between the immobilized GOx and the electrode. The results clearly demonstrate that the produced film (OOPPy-nanoAu) is an excellent biocompatible template for the immobilization of GOx and for the fabrication of glucose biosensor. The proposed glucose biosensor exhibited excellent electrochemical characteristics and high analytical performance in terms of speed, sensitivity, stability, selectivity, linear range and limit of detection.

2. Experimental

2.1. Reagents and chemicals

All chemicals were of analytical reagent grade and used without further purification except for pyrrole (Py). Glucose, pyrrole, KH_2PO_4, H_2SO_4, Na_2SO_4, KOH, KCl, HCl, CH_3COONa, $K_3[Fe(CN)_6]$ and $K_4[Fe(CN)_6]$ were obtained from Merck (Darmstadt, Germany). Glucose oxidase (GOx, EC 1.1.3.4, type VII from Aspergillus niger, 221 U mg^{-1}), D-(+)-glucose (97%) and tetrachloroauric(III) acid ($HAuCl_4 \cdot 3H_2O$) were obtained from Sigma (St. Louis, MO, USA). Pyrrole was purified twice by distillation under nitrogen atmosphere. Ten milligram of GOx was dissolved in 1 mL of acetate buffer (0.1 M and pH 5.5) to prepare a 10 mg mL^{-1} of GOx working solution. A stock solution of glucose (1 M) was prepared in doubly distilled water and stored at 4 °C when not in use. The stock solution of glucose was allowed to mutarotate at room temperature for 24 h before use. 0.1 M KH_2PO_4 was used to prepare phosphate buffer solution (PBS) and its pH was adjusted at 7.0 using KOH solution. Double distilled water was used throughout.

2.2. Apparatus

Cyclic voltammetry and amperometric studies were performed using an Autolab potentiostat-galvanostat model PGSTAT30 (Utrecht, The Netherlands) with a conventional three-electrode setup, in which a GCE/OOPPy-nanoAu/GOx, an $Ag|AgCl|KCl_{sat}$ and a platinum rod served as the working, reference and auxiliary electrodes, respectively. The working potential was applied in the standard way using the potentiostat and the output signal was acquired by Autolab Nova (version 1.7) software. All measurements were performed at room temperature.

2.3. Fabrication of glucose biosensor (GCE/OOPPy-nanoAu/GOx)

The end surface of a GCE (i.d. = 3.0 mm, Metrohm, Herisau, Switzerland) was polished on a synthetic cloth successively with 0.3, 0.1 and 0.05 μm alumina slurry (Struers, Copenhagen, Denmark) to obtain a mirror finish and then cleaned in water–ethanol solution (1:1) under ultrasonication. A freshly polished GCE was immersed in a 0.1 M H_2SO_4 solution containing Py (0.05 M) and Na_2SO_4 (0.1 M). Cyclic voltammetry was performed in a potential range between −0.3 and 0.8 V versus $Ag|AgCl|KCl_{sat}$ at a scan rate of 20 mV s^{-1} for a period of three cycles to electropolymerize Py on the surface of GCE. The modified electrode (GCE/PPy) was then rinsed thoroughly with water and transferred into a voltammetric cell containing 0.1 M NaOH solution. The conductive PPy film at surface of the GCE was electrochemically overoxidized to OOPPy by applying potential of +1.0 V versus $Ag|AgCl|KCl_{sat}$ for 300 s. The obtained electrode (GCE/OOPPy) was washed with water and immersed in a 0.1 mM $HAuCl_4$ solution containing 0.1 M KCl. The gold nanoparticles were electrochemically deposited on GCE/OOPPy using cyclic voltammetry by applying potential between 0.2 and −1.0 V versus $Ag|AgCl|KCl_{sat}$ at a scan rate of 50 mV s^{-1} for 20 cycles. The decorated GCE/OOPPy with Au NPs was denoted as GCE/OOPPy-nanoAu. The prepared electrode (GCE/OOPPy-nanoAu) was immersed in a GOx working solution (10 mg mL^{-1}, 0.1 M acetate buffer and pH 5.5) for about 24 h at 4 °C to immobilize GOx on the electrode surface. Finally, the fabricated glucose biosensor (GCE/OOPPy-nanoAu/GOx) was rinsed thoroughly with water to wash away the loosely adsorbed enzyme molecules. The fabricated glucose biosensor was stored at 4 °C in refrigerator when not in use. For comparison GCE/PPy-nanoAu and GCE/PPy-nanoAu/GOx were prepared through similar procedures.

3. Results and discussion

3.1. Characterization of GCE/OOPPy-nanoAu

SEM image of a OOPPy modified GCE showed the formation of polymer film at the surface of GCE with an organized wrinkled pattern (Fig. 1a and b). Electrochemical reduction of auric ions (Au^{+3}) on GCE/OOPPy caused the formation of Au nanoparticles on the surface of the polymer with a diameter less than 200 nm (Fig. 1c and d). Electrochemical impedance spectroscopy was employed to investigate the charge transfer property of $Fe(CN)_6^{3-/4-}$ redox couple at the investigated electrodes. The Nyquist plot of the EIS includes a semicircular portion at high frequencies which corresponds to the electron-transfer limited process and a linear portion at low frequencies which corresponds to the diffusion limited process. The diameter of semicircular portion is equal to the charge transfer resistance (R_{ct}) which shows the kinetic of electron transfer of the redox probe at the electrode interface. Fig. 2 displays the Nyquist plots obtained for a GCE (a), GCE/OOPPy (b) and GCE/OOPPy-nanoAu (c) in a solution containing 5.0 mM $Fe(CN)_6^{3-/4-}$ couple (1:1) and 0.1 M KCl. The semicircular diameter

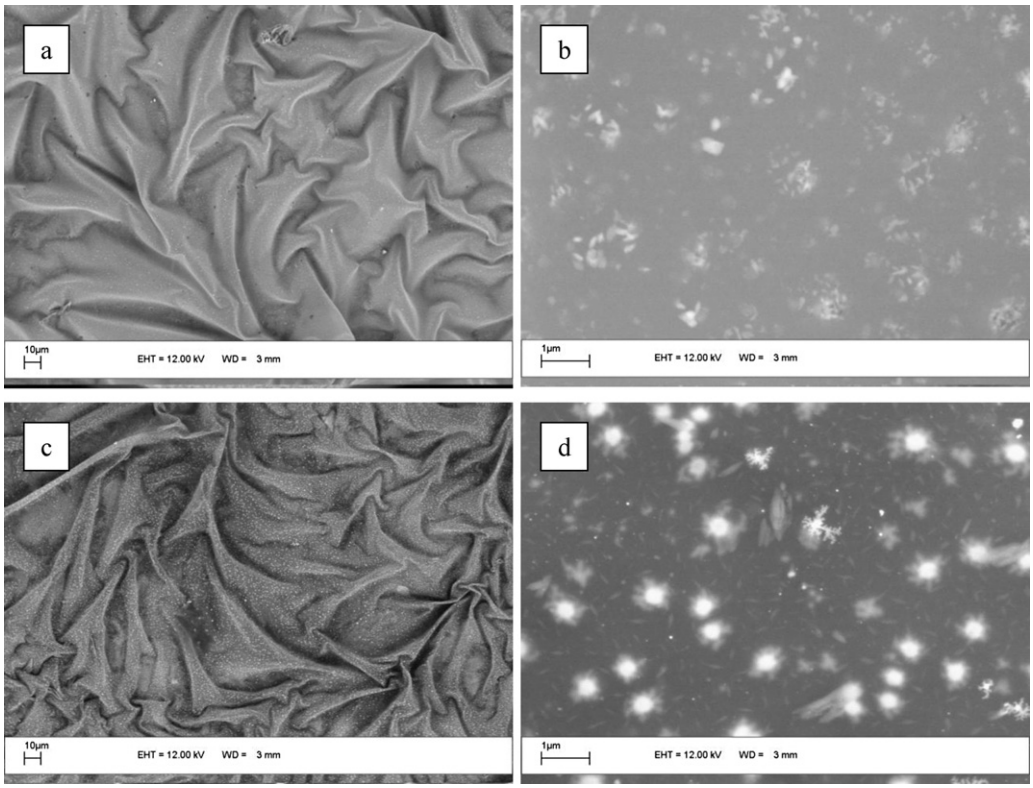

Fig. 1. SEM images of a GCE/OOPPy (a and b) and a GCE/OOPPy-nanoAu (c and d).

(R_{ct}) of GCE/OOPPy-nanoAu was much less than those observed for GCE and GCE/OOPPy, suggesting that decorated Au NPs facilitated the rate of electron transfer of the redox probe at the modified electrode interface. Also, cyclic voltammetry studies showed (Fig. 2, inset) that the observed peak to peak separation for $Fe(CN)_6^{3-/4-}$ redox couple on GCE/OOPPy-nanoAu (87 mV) was less than those observed for GCE (132 mV) and GCE/OOPPy (117 mV), verifying the results obtained by EIS.

Cyclic voltammetry (CV) was performed using a GCE/OOPPy-nanoAu at different scan rates in a solution containing 5 mM $Fe(CN)_6^{3-/4-}$ redox couple (1:1) and 0.1 M KCl to estimate the apparent surface area (A) of a GCE/OOPPy-nanoAu. The estimated value for A, calculated from the slope of the plot of peak current (I_p) versus square root of scan rate ($\nu^{1/2}$) at T = 298 K (25 °C) according to the Randles-Sevcik equation [36] was 0.071 cm^2.

3.2. Electrochemical behavior of GCE/OOPPy-nanoAu/GOx

Fig. 3 shows cyclic voltammograms of a GCE/OOPPy-nanoAu, GCE/OOPPy-nanoAu/GOx and GCE/PPy-nanoAu/GOx in a N_2-saturated PBS pH of 7.0 at a scan rate of 50 mV s^{-1}. A couple of well-defined redox peaks was observed for the immobilized GOx on GCE/OOPPy-nanoAu/GOx (Fig. 3, solid line) and no redox peaks for GCE/OOPPy-nanoAu (Fig. 3, dashed line). There was also no obvious redox peaks for the immobilized GOx on GCE/PPy-nanoAu/GOx (Fig. 3, inset). It is well-known that the active redox

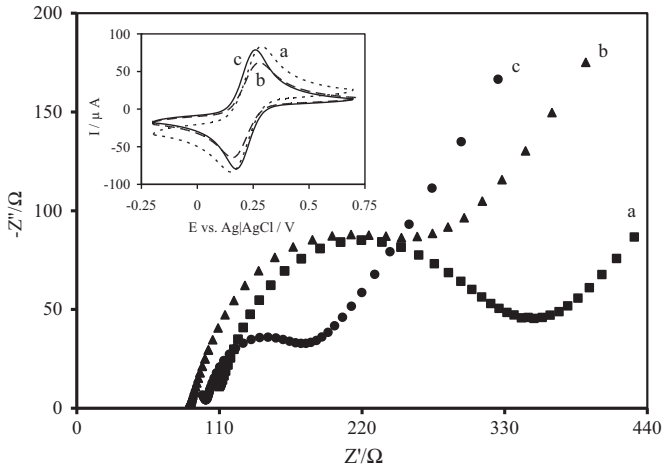

Fig. 2. Nyquist plots and cyclic voltammograms (the inset) for a GCE (a), GCE/OOPPy (b) and GCE/OOPPy-nanoAu (c) in a solution containing 5.0 mM $Fe(CN)_6^{3-/4-}$ couple (1:1) and 0.1 M KCl. Scan rate for cyclic voltammetry studies was 100 mV s^{-1}.

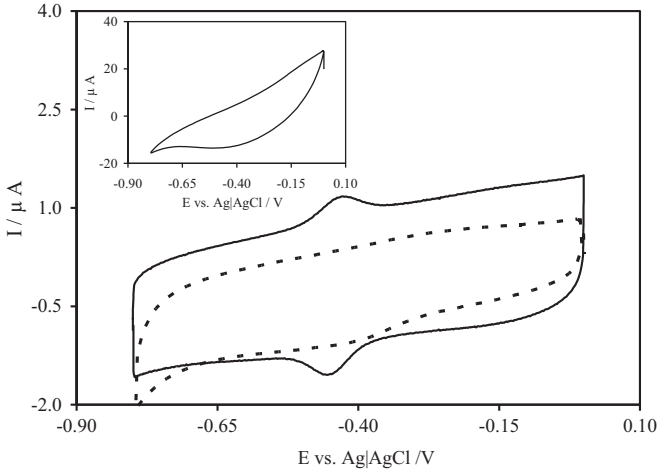

Fig. 3. Cyclic voltammograms of a GCE/OOPPy-nanoAu/GOx (solid line), GCE/OOPPy-nanoAu (dashed line) and GCE/PPy-nanoAu/GOx (the inset) in a N_2-saturated PBS (0.1 M and pH 7.0) at a scan rate of 50 mV s^{-1}.

center of GOx, flavin adenine dinucleotide (FAD), is deeply embedded in a protective protein shell, which makes the direct electron communication with electrode extremely difficult. But, the results showed that OOPPy-nanoAu compared with PPy-nanoAu provided an excellent biocompatible medium with an extraordinary electron transport property for achieving direct electron transfer between GOx and medium. The observed anodic (E_{pa}), cathodic (E_{pc}) and formal ($E^{\circ\prime} = (E_{pc} + E_{pa})/2$) peak potentials for the immobilized GOx on GCE/OOPPy-nanoAu/GOx were −0.435, −0.463 and −0.449 V, respectively. Also, the value of peak-to-peak separation ($\Delta E_p = E_{pa} - E_{pc}$) and the ratio of cathodic (I_{pc}) to anodic (I_{pa}) peak current intensities were 28 mV and 1, respectively.

Cyclic voltammograms of a GCE/OOPPy-nanoAu/GOx were recorded in a N_2-saturated PBS at pH of 7.0 and different scan rates (ν). The results indicated that the peak current intensities (I_p) increased linearly with the scan rate in the range between 10 and 1000 mV s^{-1}, revealing a surface-limited redox process (Fig. S1). The surface concentration (Γ_c) of the electroactive GOx was calculated from the slope I_p versus ν according to equation (1) [37] derived for a reversible surface redox reaction:

$$I_p = \frac{n^2F^2A\nu\Gamma_c}{4RT} \quad (1)$$

where A is the apparent surface area and the other symbols have their usual meanings. The value of Γ_c was 6.18×10^{-11} mol cm^{-2} for $n = 2$ and $A = 0.071$ cm^2. The obtained value for Γ_c was larger than that reported for gold nanoparticles modified carbon paste electrode (9.8×10^{-12} mol cm^{-2}) [38].

Supplementary material related to this article found, in the online version, at http://dx.doi.org/10.1016/j.colsurfb.2012.11.010.

Based on the Laviron theory [39] the apparent heterogeneous electron transfer rate constant (k_s) was determined for the immobilized GOx on a GCE/OOPPy-nanoAu/GOx in a N_2-saturated PBS at pH of 7.0 by measuring the variation of peak potentials at different scan rates. The observed peak-to-peak separations (ΔE_p) at different scan rates between 10 and 1000 mV s^{-1} were smaller than 200/n mV wherein $n = 2$. The obtained average value for k_s was 10.3 s^{-1}, assuming $\alpha = 0.5$. It noted that the relative error in k_s is at the most 6% if $\alpha = 0.5$ is used. The observed k_s was higher than the value observed for the immobilized GOx on the colloidal gold nanoparticles in Nafion film (1.30 s^{-1}) [40], the carbon nanotube electrode (1.5 s^{-1}) [41], the amine-terminated ionic liquid functionalized carbon nanotube–gold nanoparticles (2.12 s^{-1}) [42], the graphene-chitosan modified electrode (3.01 s^{-1}) [43], the gold nanoparticles electrodeposited on an indium tin oxide electrode (3.7 s^{-1}) [44], the GCE modified with Nafion and mesoporous carbon FDU-15 (4.095 s^{-1}) [45], the ordered mesoporous carbon–Au nanoparticles (OMC–Au) nano-hybrid modified electrode (5.03 s^{-1}) [46] and the nano-porous glassy carbon electrode (5.27 s^{-1}) [47].

It seems that a medium with an excellent electrical conductivity and extraordinary electron transport property is provided by OOPPy-nanoAu film (Fig. 2). The enhancement of the mentioned properties can be attributed to the presence of Au NPs in the hybrid. Also, an excellent biocompatible medium for GOx immobilization is provided by OOPPy-nanoAu (Fig. 3). Therefore, it seems that OOPPy provides an excellent biocompatible template for the immobilization of GOx and the presence of Au NPs in the prepared hybrid, OOPPy-nanoAu, enhances the electrical conductivity and electron transport property of the hybrid. It seems in addition to the excellent electrical conductivity, extraordinary electron transport property and excellent template biocompatibility, the efficient interaction between OOPPy-nanoAu and the immobilized GOx causes to observe a superior electron transfer rate constant ($k_s = 10.3$ s^{-1}).

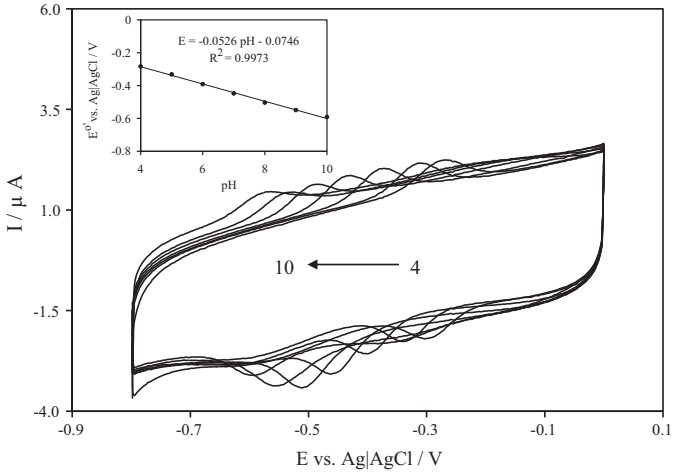

Fig. 4. Cyclic voltammograms of a GCE/OOPPy-nanoAu/GOx in a N_2-saturated PBS (0.1 M) with different pHs from 4.0 to 10.0 at a scan rate of 50 mV s^{-1}. Inset: plot of formal potential ($E^{\circ\prime}$) versus pH.

The reduction of flavin adenine dinucleotide (FAD), the active redox center of GOx, is accompanied by protonation; therefore the pH of solution has a significant effect on the electrochemical behavior of FAD. In order to explore the effect of pH on the electrochemical behavior of the immobilized GOx on GCE/OOPPy-nanoAu/GOx, cyclic voltammetry was employed in a N_2-saturated PBS at different pHs to measure the variation of the formal peak potential ($E^{\circ\prime}$) with pH. As shown in Fig. 4, clear voltammograms with well-defined redox peaks were observed at different pHs ranging from 4 to 10; however, the voltammograms shifted to more negative potentials with increasing pH. The plot of $E^{\circ\prime}$ versus pH ranging from 4 to 10 (Fig. 4, inset) yielded a straight line with a slope equal to −52.6 mV pH^{-1} at 25 °C, which was close to the theoretical value of −58.6 mV pH^{-1} for a $2e^-/2H^+$ redox process.

Cyclic voltammograms of a GCE/OOPPy-nanoAu/GOx (Fig. 5) and a GCE/OOPPy-nanoAu (Fig. 5, inset) in N_2-saturated and O_2-saturated phosphate buffer solutions (0.1 M and pH 7.0) revealed the excellent electrocatalytic activity of the GCE/OOPPy-nanoAu toward the reduction of O_2. It is likely that the observed electrocatalytic activity toward O_2 reduction originates from the extraordinary electron transport property of the OOPPy-nanoAu film.

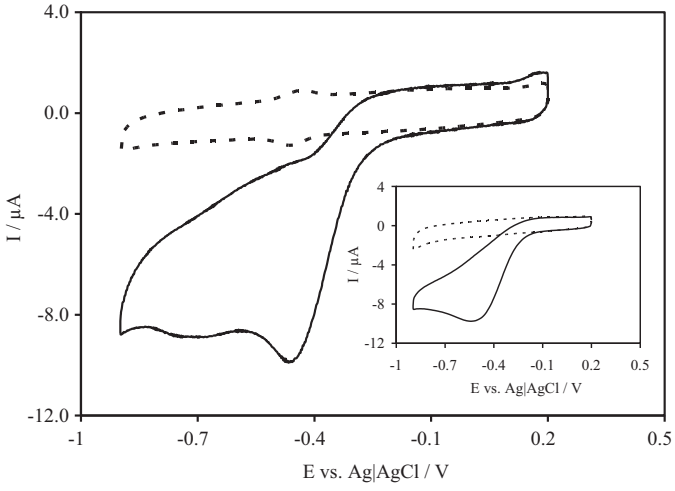

Fig. 5. Cyclic voltammograms of a GCE/OOPPy-nanoAu/GOx and a GCE/OOPPy-nanoAu (the inset) in N_2-saturated (dashed line) and O_2-saturated (solid line) PBS (0.1 M and pH 7.0) at a scan rate of 20 mV s^{-1}.

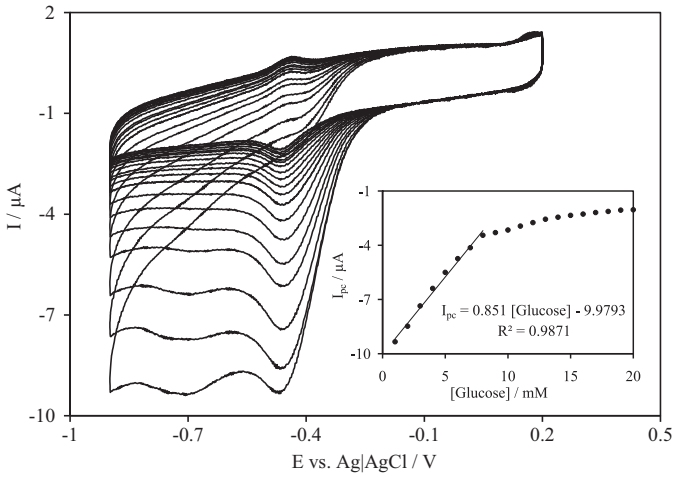

Fig. 6. Cyclic voltammograms of a GCE/OOPPy-nanoAu/GOx in a O_2-saturated PBS (0.1 M and pH 7.0) containing different amounts of glucose from 1 to 20 mM (from outer to inner with 1 mM increments) at scan rate of 20 mV s^{-1}. Inset, plot of the reduction peak current (I_{pc}) of oxygen versus concentration of glucose.

3.3. Electrochemical behavior of GCE/OOPPy-nanoAu/GOx toward glucose

Cyclic voltammograms for a series of standard glucose solutions were recorded in a O_2-saturated PBS (0.1 M and pH 7.0) using the proposed biosensor (GCE/OOPPy-nanoAu/GOx). As shown in Fig. 6 the current signal intensity due to the reduction of oxygen which is started at about −150 mV versus Ag|AgCl|KCl_{sat} decreases with increasing the concentration of glucose, indicating the consumption of oxygen during the course of the enzymatic reaction of GOx with glucose (Eq. (2)).

$$\text{Glucose} + \text{GOx-FAD} + O_2 \rightarrow \text{GOx-FAD} + \text{Gluconolactone} + H_2O_2 \quad (2)$$

The inset in Fig. 6 shows the plot of the reduction peak current intensity (I_{pc}) of oxygen at different concentrations of glucose. Also, the proposed glucose biosensor was employed for the amperometric determination of glucose. Fig. 7 depicts a current-time plot of the biosensor recorded for the successive additions of glucose solution in a O_2-saturated PBS (0.1 M and pH 7.0) at the applied potential of −0.4 V versus Ag|AgCl|KCl_{sat}. As shown in Fig. 7 the reduction current responses of the biosensor decrease with increasing glucose concentration. The response time of the biosensor toward glucose was about 11 s. Fig. 7, the inset shows the plot of amperometric response of the biosensor at different concentrations of glucose. The calibration curve for glucose determination using both cyclic voltammetry and amperometry was linear between 1 and 8 mM. The sensitivity of the biosensor toward glucose using cyclic voltammetry and amperometry was 0.851 and 0.217 μA mM^{-1}, respectively. Also, the limit of detection (S/N = 3) using cyclic voltammetry and amperometry was 0.7 and 0.5 mM, respectively. The relative standard deviation for repetitive measurements (n = 6) of 5 mM glucose using cyclic voltammetry was 2.4%.

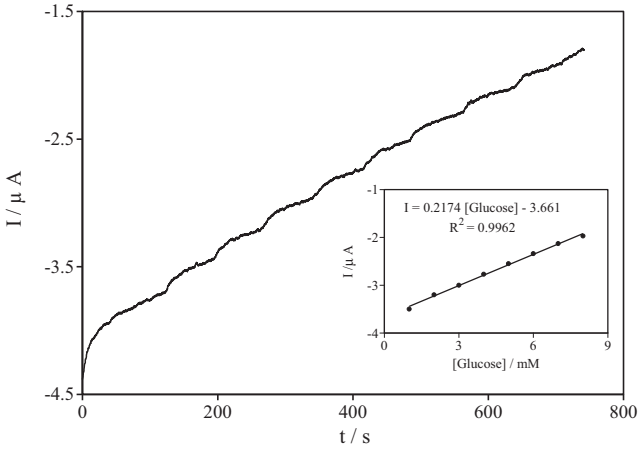

Fig. 7. Hydrodynamic amperometric responses for a GCE/OOPPy-nanoAu/GOx in a O_2-saturated PBS (0.1 M and pH 7.0) to successive additions of 1 mM glucose. Inset, plot of amperometric response versus concentration of glucose. Operating potential: −400 mV versus Ag|AgCl|KCl_{sat}.

The operational stability of the proposed glucose biosensor was examined by monitoring of its voltammetric currents during potential cycling in a O_2-saturated PBS (0.1 M and pH 7.0). No significant decrease was observed in voltammetric currents of the biosensor by recycling potential for 30 cycles in potential range between 0.2 and −0.9 V with a scan rate of 50 mV s^{-1}. After storing the biosensor in a N_2-saturated PBS (0.1 M and pH 7.0) at 4 °C for 2 weeks, its voltammetric current decreased by approximately 8.2%. This exceptional stability can be attributed to the biocompatibility of the OOPPy-nanoAu film which can provide a suitable environment for GOx immobilization.

The effect of the presence of three possible interfering substances; uric acid, ascorbic acid and acetaminophen; on the response of the biosensor toward 1 mM glucose was examined to evaluate the selectivity of the proposed biosensor. Amperometry was performed in a O_2-saturated PBS (0.1 M and pH 7.0) in the presence (0.5 mM) and absence of interfering substances. A 5% error criterion was adopted. No obvious interference was observed from the mentioned substances at the concentration of 0.5 mM.

Normally, the blood glucose level is maintained between about 4 and 6 mM. So, the linear glucose response from 1 to 8 mM based on the proposed glucose biosensor is enough and suitable for its practical application in determining blood glucose concentration. So, the proposed glucose biosensor was employed for the determination of glucose in normal human serum to examine its applicability for real sample analysis. A 200 μL of normal human serum was mixed with 1.8 mL O_2-saturated PBS (0.1 M and pH 7.0) and then analyzed using amperometry and applying the proposed biosensor. The concentration of glucose in normal human serum was determined to be 5.46 mM. The recovery of the analysis was about 103%, considering the value determined by a local hospital (5.30 mM). Also, to examine the reliability of the proposed biosensor, 200 μL of the normal human serum was mixed with a 1.8 mL O_2-saturated PBS (0.1 M and pH 7.0) containing specific amounts of glucose (0, 0.5, 1.0, 1.5, 2.0, 2.5 and 3.0 mM) and was then analyzed using amperometry. The recovery for each measurement was calculated by comparing the results obtained in the absence and presence of specific amounts of glucose. The obtained average recovery for the spiked samples was 96%.

4. Conclusions

An electrochemically prepared OOPPy film on the surface of a GCE was decorated with Au nanoparticles to prepare OOPPy-nanoAu film on the surface of a GCE. Glucose oxidase was then immobilized on the surface of OOPPy-nanoAu by physical adsorption. Cyclic voltammetry in a N_2-saturated phosphate buffer solution showed a pair of well-defined redox peaks as a result of direct electron transfer between the GOx and OOPPy-nanoAu. The results indicated that the OOPPy-nanoAu film provided a biocompatible scaffold with an excellent electrical conductivity and extraordinary electron transport property for the efficient

interaction between the GOx and the medium. The electron transfer rate constant for the immobilized GOx on OOPPy-nanoAu film was superior to those reported previously ($k_s = 10.3\ s^{-1}$). Also, an excellent electrocatalytic activity toward the reduction of O_2 was observed for the prepared OOPPy-nanoAu hybrid. The proposed biosensor was employed for glucose detection using both cyclic voltammetry and amperometry on the basis of the excellent electrocatalytic activity of the OOPPy-nanoAu film toward the reduction of O_2. The linear response of the fabricated biosensor toward glucose from 1 to 8 mM was suitable for its practical application in determining blood glucose concentration without any pretreatment. The proposed biosensor was successfully applied for the determination of glucose in blood sample with satisfactory results. Additionally, the proposed glucose biosensor exhibited a fast amperometric response time (11 s), high operational and storage stabilities and high selectivity.

Acknowledgements

The authors acknowledge the Institute for Advanced Studies in Basic Science (IASBS, grant number G2102IASBS119) and the Iran National Science Foundation (INSF, grant number 90003581) for the financial supports.

References

[1] X. Zhang, H. Ju, J. Wang, Electrochemical Sensors Biosensors and their Biomedical Applications, Elsevier, Amsterdam (The Netherlands), 2008.
[2] M. Gerard, A. Chaubey, B.D. Malhotra, Biosens. Bioelectron. 17 (2002) 345–359.
[3] M.A. Rahman, P. Kumar, D.-S. Park, Y.-B. Shim, Sensors 8 (2008) 118–141.
[4] A. Malinauskas, R. Garjonytimage, R. Maimageeikien, Talanta 64 (2004) 121–129.
[5] B.A. Gregg, A. Heller, J. Phys. Chem. 95 (1991) 5976–5980.
[6] C.A.P. Quinn, R.E. Connor, A. Heller, Biomaterials 18 (1997) 1665–1670.
[7] B.F.Y. Yon-Hin, M. Smolander, T. Crompton, C.R. Lowe, Anal. Chem. 65 (1993) 2067–2071.
[8] L.H. Eng, M. Elmgren, P. Komlos, M. Nordling, S.-E. Lindquist, H.Y. Neujahr, J. Phys. Chem. 98 (1994) 7068–7072.
[9] S. Geetha, C.R.K. Rao, M. Vijayan, D.C. Trivedi, Anal. Chim. Acta 568 (2006) 119–125.
[10] S. Szunerits, L. Bouffier, R. Calemczuk, B. Corso, M. Demeunynck, E. Descamps, Y. Defontaine, J.-B. Fiche, E. Fortin, T. Livache, P. Mailley, A. Roget, E. Vieil, Electroanalysis 17 (2005) 2001–2017.
[11] C.M. Li, C.Q. Sun, W. Chen, L. Pan, Surf. Coat. Technol. 198 (2005) 474–477.
[12] S. Rapi, V. Bocchi, G.P. Gardini, Synth. Met. 24 (1988) 217–221.
[13] M.M. Castillo-Ortega, M.B. Inouea, M. Inoue, Synth. Met. 28 (1989) 65–70.
[14] V. Bocchi, G.P. Gardini, J. Chem. Soc. Chem. Commun. 1 (1986), 148a–148a.
[15] S. Wencheng, J.O. Iroh, Synth. Met. 95 (1998) 159–167.
[16] N. Balci, E. Bayramli, L. Toppare, J. Appl. Polym. Sci. 64 (1997) 667–671.
[17] S.N. Mailu, T.T. Waryo, P.M. Ndangili, F.R. Ngece, A.A. Baleg, P.G. Baker, E.I. Iwuoha, Sensors 10 (2010) 9449–9465.
[18] X. Jiang, X. Lin, Analyst 130 (2005) 391–396.
[19] A. Witkowski, A. Brajter-Toth, Anal. Chem. 64 (1992) 635–641.
[20] R.B. Rakhi, K. Sethupathi, S. Ramaprabhu, J. Phys. Chem. B 113 (2009) 3190–3194.
[21] J.-C. Vidal, E. Garcia, J.-R. Castillo, Biosens. Bioelectron. 13 (1998) 371–382.
[22] G. Fortier, E. Brassard, D. Belanger, Biosens. Bioelectron. 5 (1990) 473–490.
[23] G.E. De Benedetto, F. Palmisano, P.G. Zambonin, Biosens. Bioelectron. 11 (1996) 1001–1008.
[24] M.-C. Shin, H.-S. Kim, Biosens. Bioelectron. 11 (1996) 161–169.
[25] M. Zhu, Z. Jiang, W. Jing, Sens. Actuators B: Chem. 110 (2005) 382–389.
[26] J. Wang, N.V. Myung, M. Yun, H.G. Monbouquette, J. Electroanal. Chem. 575 (2005) 139–146.
[27] E.M.I.M. Ekanayake, D.M.G. Preethichandra, K. Kaneto, Biosens. Bioelectron. 23 (2007) 107–113.
[28] D. Olea, P. Moreau, C. Faure, J. Electroanal. Chem. 605 (2007) 125–135.
[29] M. Singh, P.K. Kathuroju, N. Jampana, Sens. Actuators B: Chem. 143 (2009) 430–443.
[30] A. Kausaite-Minkstimiene, V. Mazeiko, A. Ramanaviciene, A. Ramanavicius, Sens. Actuators B: Chem. 158 (2011) 278–285.
[31] J. Li, X. Lin, Biosens. Bioelectron. 22 (2007) 2898–2905.
[32] J. Njagi, S. Andreescu, Biosens. Bioelectron. 23 (2007) 168–175.
[33] A. Guerrieri, G.E. De Benedetto, F. Palmisano, P.G. Zambonin, Biosens. Bioelectron. 13 (1998) 103–112.
[34] L. Özcan, Y. Sahin, H. Türk, Biosens. Bioelectron. 24 (2008) 512–517.
[35] C. Debiemme-Chouvy, G. Navarro, ECS Trans. 33 (2011) 21–24.
[36] A.J. Bard, L.R. Faulkner, Electrochemical Methods, Fundamentals and Applications, 2nd ed., Wiley, New York, 2001.
[37] J. Wang, Analytical Electrochemistry, 3rd ed., VCH, New York, 2006.
[38] S. Liu, H. Ju, Biosens. Bioelectron. 19 (2003) 177–183.
[39] E. Laviron, J. Electroanal. Chem. 101 (1979) 19–28.
[40] S. Zhao, K. Zhang, Y. Baia, W. Yang, C. Sun, Bioelectrochemistry 69 (2006) 158–163.
[41] C. Cai, J. Chen, Anal. Biochem. 332 (2004) 75–83.
[42] R. Gao, J. Zheng, Electrochem. Commun. 11 (2009) 608–611.
[43] X.H. Kang, J. Wang, H. Wu, I.A. Aksay, J. Liu, Y.H. Lin, Biosens. Bioelectron. 25 (2009) 901–905.
[44] J. Wang, L. Wang, J. Di, Y. Tu, Sens. Actuators B: Chem. 135 (2008) 283–288.
[45] K. Wang, H. Yang, L. Zhu, Z. Ma, S. Xing, Q. Lv, J. Liao, C. Liu, W. Xing, Electrochim. Acta 54 (2009) 4626–4630.
[46] L. Wang, J. Bai, X. Bo, X. Zhang, L. Guo, Talanta 83 (2011) 1386–1391.
[47] B. Haghighi, M.A. Tabrizi, Electrochim. Acta 56 (2011) 10101–10106.